Clays and Clay Minerals, Vol. 32, No. 5, 363–374, 1984.

WEATHERING OF ILMENITE IN A LATERITIC PALLID ZONE

R. R. ANAND AND R. J. GILKES

Department of Soil Science and Plant Nutrition, University of Western Australia
Nedlands, Western Australia 6009, Australia

Abstract—In a lateritic pallid zone ilmenite crystals alter via pseudorutile to porous leucoxene grains composed of randomly oriented aggregates of ~0.06 μm anatase crystals. This style of alteration differs from that in beach sands where parallel oriented rutile crystals develop from pseudorutile. Increased Si and Al in the altered grains is due to the crystallization from soil solution of halloysite, kaolinite and gibbsite within pores rather than to the incorporation of these elements into anatase crystals. Manganese was a significant constituent (3.2% Mn_2O_3) of the original ilmenite but was not retained by the leucoxene grains. The minor constituents Ni, Zn, Cu, Mg, Co and Ca were also lost, but Cr and V were retained.

Key Words—Anatase, Halloysite, Ilmenite, Kaolinite, Laterite, Leucoxene, Pseudorutile, Rutile, Weathering.

INTRODUCTION

The weathering of ilmenite is not well understood and deserves further investigation. It has been reported to alter to various products including anatase, rutile, a noncrystalline iron titanate (Bailey *et al.*, 1956); arizonite (Palmer, 1909; Karkhanavala, 1959); hydroilmenite (Flinter, 1959); proarizonite (Bykov, 1964), and pseudorutile (Teufer and Temple, 1966; Grey and Reid, 1975). The relationship of the weathering environment and the nature of the alteration products of ilmenite is also not known. The alteration of ilmenite in beach sand ore bodies has been extensively studied due to its economic importance, but relatively little attention (Hartman, 1959; Van Houten, 1968) has been given to the stability of this mineral in other soil environments. Hartman (1959) considered that the alteration mechanism of ilmenite during bauxitization is different from that in weathered beach sands and that three distinct types of alteration occurred in bauxites: (1) direct alteration to leucoxene; (2) direct alteration to optically identifiable anatase; (3) alteration to "patchy" ilmenite.

The weathering of ilmenite in soils is of considerable interest to geologists because this mineral is a major primary source of the Ti in soils. Furthermore, the form of Ti in soils is to some extent determined by the alteration processes occurring within the confines of a single ilmenite grain rather than in the general soil matrix. Ilmenite commonly contains significant substitutions of Mn, Mg, V, Cr (Deer *et al.*, 1962), so that its mode of alteration will also affect the concentration and form of these elements in some soils. These considerations suggest that there is clearly a need for a better understanding of weathering of ilmenite in soils. This paper deals with mineralogical and chemical aspects of ilmenite weathering in the pallid zone of a laterite developed from dolerite in southwestern Australia.

MATERIALS AND METHODS

Samples from a laterite pallid zone developed from metamorphosed quartz dolerite were collected from a railway cutting at Jarrahdale, 45 km southeast of Perth, Western Australia. Detailed profile descriptions of the deeply weathered lateritic soil profile at this site were given by Sadleir and Gilkes (1976). The profile contains a distinct sequence of horizons, i.e., parent material (deeper than 10 m and not exposed), mottled, red-white pallid-zone clay (depth interval, 6–10 m), irregular, brown, nodular concretions (4–6 m), loose, brown, nodular hard cap (2–4 m), and pisolitic hard cap (0–2 m). Altered ilmenite grains were separated from the bulk samples which had been disaggregated by gentle shaking in 0.1 M NaOH solution. Partially and highly altered (leucoxene) grains remained intact and were next separated from other mineral grains in a Frantz isodynamic magnetic separator.

X-ray powder diffraction (XRD) patterns of bulk samples of altered grains separated from the pallid zone were obtained with a Philips diffractometer with Fe-filtered CoKα radiation. For the measurement of the unit-cell parameters a CaF_2 internal standard was added, and the powdered sample was scanned at a rate of 0.25°2θ/min. Single-grain X-ray diffraction patterns were made using a Gandolfi single crystal camera (Gandolfi, 1967). Semiquantitative analysis of the minerals in the pallid-zone clay was made by thermogravimetric analysis (TGA). Simultaneous TGA and differential thermogravimetric (DTGA) curves for 10-mg samples were obtained in flowing air at a heating rate of 10°C/min using a Perkin Elmer TG 52 instrument. Dehydration maxima at 60, 280, and 500°C produced by halloysite(10Å), gibbsite, and halloysite(7Å) + kaolinite, respectively, were used to estimate the concentration of these minerals.

Polished sections of bulk pallid-zone clay samples and ilmenite concentrates were made for petrographic

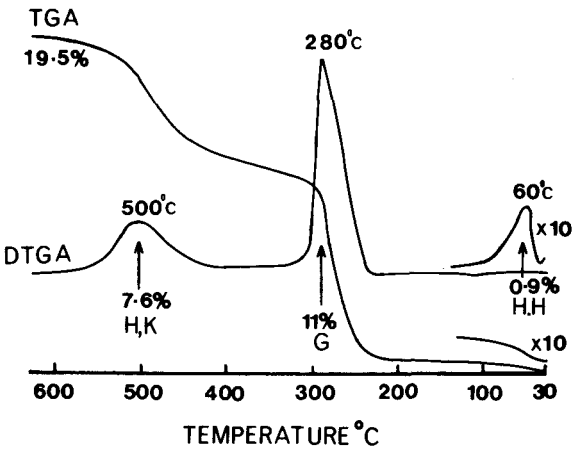

Figure 1. Thermogravimetric curves for pallid-zone clay. DTGA = differential thermal gravimetric analysis; TGA = thermogravimetric analysis; HH = hydrated halloysite; H = halloysite; H = halloysite(7Å); K = kaolinite; G = gibbsite. Dehydration maxima at 60, 280, and 500°C correspond to hydrated halloysite, gibbsite, and halloysite(7Å) + kaolinite, respectively. The values 0.9%, 11%, and 7.6% are water losses due to hydrated halloysite, gibbsite, and halloysite(7Å) + kaolinite, respectively, and account for the total 19.5% water loss.

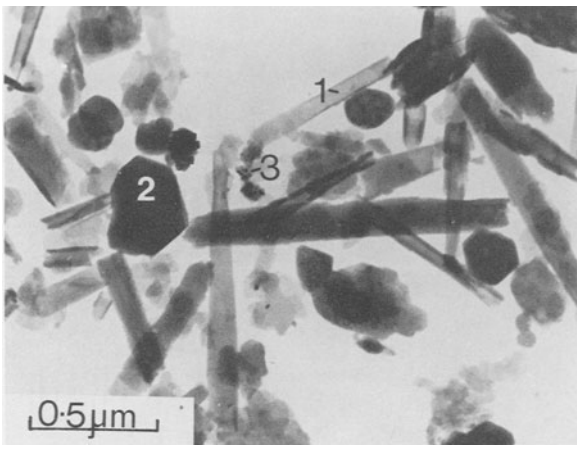

Figure 2. Transmission electron micrograph of the clay (<2 μm) fraction of pallid-zone clay showing tubular halloysite crystals (1); platy crystals of kaolinite or gibbsite (2), and aggregates of very small (~0.02 μm) anatase crystals (3).

and electron microprobe examination. Separated grains were mounted on aluminum stubs and coated with a 150-Å layer of platinum in a vacuum evaporator and investigated by scanning electron microscopy (SEM) using a Philips PSEM 500 instrument. Selected grains were crushed and dispersed for transmission electron microscopy (TEM) and selected area electron diffraction (SAD) using a Hitachi HU11B instrument. Pallid-zone samples and subsamples of highly altered grains were analyzed for major and trace elements by X-ray fluorescence spectrometry after fusion in a lithium borate–lithium carbonate flux (low dilution fusion) following the method of Lee and McConchie (1982). Subsamples of partially altered grains were dissolved in a mixture of $HClO_4$ and HF acids and analyzed for Ti, Fe, Mn, Ca, Al, Si, Cr, Ni, Zn, V, Cu, Mg, and Co using a Perkin Elmer atomic absorption spectrophotometer. Ferrous iron was determined under a nitrogen atmosphere by dichromate titration (Vogel, 1961). Chemical analyses of different phases within grains viz. ilmenite, pseudorutile, and anatase were obtained from polished sections using an ARL-SEMQ electron microprobe.

RESULTS AND DISCUSSION

XRD patterns of bulk samples showed that halloysite, kaolinite, gibbsite, quartz, ilmenite, and anatase were present in the pallid-zone clay. TGA of bulk pallid-zone samples showed the presence of about 6% halloysite(10Å), 46% halloysite(7Å) and/or kaolinite, and 32% gibbsite (Figure 1). TGA of replicate samples and standard mixtures showed a lower limit of detection of 2% and a reproducibility of 2% for these minerals. The chemical composition of the bulk pallid-zone clay is shown in Table 1 and corresponds well with the mineralogy determined by XRD and TGA. The distribution of Ti between the various materials was estimated on the basis of chemical analyses of these materials and microscopic measurements of their abundance. Of the 4.5% TiO_2 content of the pallid zone about 35% is in residual ilmenite, 60% is in anatase in leucoxene grains, and 5% is in microcrystalline anatase which is dispersed through clay and which has been derived from weathering of amphibole and other primary minerals. Electron micrographs of the clay fraction (<2 μm) of the pallid-zone clay show tubular halloysite crystals with an average length of 0.69 ± 0.41 μm and diameter of 0.11 ± 0.04 μm, platy kaolinite and/or gibbsite crystals with average major axis length of 0.16 ± 0.08 μm and minor axis length of 0.14 ± 0.06 μm, and aggregates of very small (~0.02 μm) anatase crystals (Figure 2). These identifications were supported by electron diffraction measurements which are described below.

XRD patterns of partially altered ilmenite grains show the presence of ilmenite, pseudorutile, and anatase (Figure 3A). Highly altered grains contained mainly anatase, traces of ilmenite and/or pseudorutile, and minor amounts of halloysite(7Å) and/or kaolinite and gibbsite (Figure 3B). X-ray diffraction patterns of non-rotated, partially altered grains taken with the Gandolfi camera showed sharp reflections of ilmenite/pseudorutile and an anatase powder pattern with no arcing of reflections, indicating that the anatase crystals were randomly oriented within the grain (Figure 4). Thus, the crystal structure of the parent ilmenite grains does not appear to control the orientation of the product

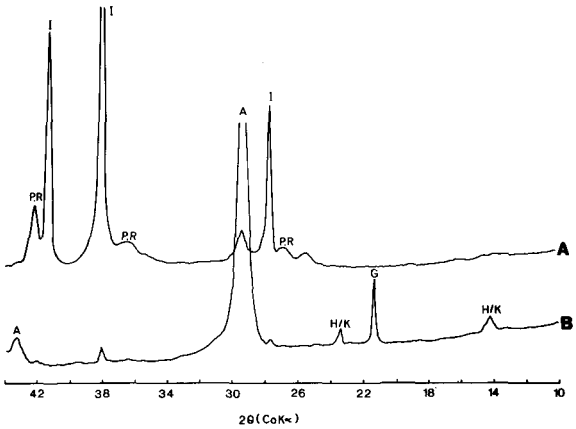

Figure 3. X-ray powder diffraction patterns of bulk samples of partially altered (A) and highly altered ilmenite (B). I = ilmenite; PR = pseudorutile; A = anatase; H/K = halloysite(7Å) and/or kaolinite; G = gibbsite.

anatase. These results are in contrast to those of Teufer and Temple (1966) and Grey and Reid (1975) who found that microcrystalline rutile in altered ilmenite grains developed as oriented aggregates by epitaxial growth upon the close-packed anion layers of ilmenite. According to Grey and Reid (1975), rutile in altered ilmenite grains is present in a triply twinned arrangement and likely resulted from dissolution followed by epitaxial growth of TiO_2. In marked contrast to the findings of these workers, we found anatase and *not* rutile to be the alteration product of the ilmenite and the overall orientation of anatase microcrystals within the altered grain to be random.

The chemical compositions of bulk samples of partially altered ilmenite and completely altered grains are shown in Table 2. Bulk samples of unweathered ilmenite grains from rock were not analyzed because unweathered dolerite containing unaltered ilmenite was

Table 1. Chemical analyses and semiquantitative mineralogical analyses based on X-ray powder diffraction and thermogravimetric analyses of pallid zone clay.

	Wt. %
SiO_2	34.3
TiO_2	4.5
Al_2O_3	38.5
Fe_2O_3	3.6
MnO	0.01
CaO	0.02
MgO	0.09
L.O.I.	19.5
Total	100.5

Halloysite and/or kaolinite = 52%
Gibbsite = 32
Quartz = 10
Ilmenite, anatase, pseudorutile = 6

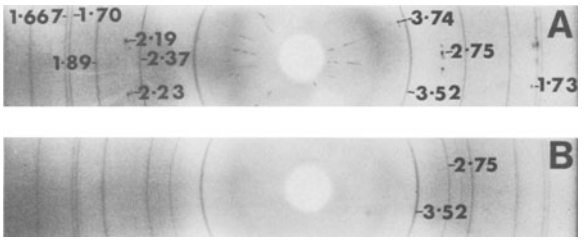

Figure 4. Gandolfi camera X-ray diffraction patterns of a single, partially altered ilmenite grain. Patterns were obtained with the grain stationary (A) and rotating (B). Spacings are indicated. 3.74 Å (102), 2.75 Å (104), 2.23 Å (113), and 1.73 Å (116) single crystal reflections correspond to ilmenite and 2.19 Å (101) to pseudorutile. 3.52 Å (101), 2.37 Å (004), 1.89 Å (200), 1.70 Å (105), and 1.667 Å (211) rings are due to anatase.

not exposed at this locality. Therefore, the ilmenite analysis in Table 2 is an average of electron microprobe analyses of unaltered parts of grains which were separated from the pallid-zone clay. The bulk sample of partially altered ilmenite consisted of a mixture of ilmenite, pseudorutile, anatase, and minor amounts of other minerals, whereas the highly altered bulk sample consisted mostly of anatase with minor amounts of ilmenite, pseudorutile and amounts of other minerals. The increase in TiO_2 in the partially altered ilmenite is accompanied by a decrease in iron to an amount that is consistent with the development of pseudorutile as a major first alteration product. During the subsequent stage of alteration, most iron was lost from completely altered grains due to dissolution of pseudorutile,

Table 2. Chemical analyses of ilmenite, partially altered ilmenite, and completely altered ilmenite (leucoxene).

Wt. %	Ilmenite[1]	Partially altered ilmenite[2]	Completely altered ilmenite[2]
FeO	44.6	19.3	—
Fe_2O_3	—	19.4	6.4
TiO_2	52.3	56.7	81.4
SiO_2	—	0.07	2.6
Al_2O_3	0.07	0.31	7.3
MnO	2.9	2.2	0.11
CaO	—	0.06	0.04
Total	99.87	98.04	97.85
ppm			
Cr	—	420	790
V	—	680	1230
Zn	—	210	70
Cu	—	160	75
Ni	—	150	60
Co	—	100	<20
Mg	—	150	25

[1] Average of electron microprobe analyses of fresh ilmenite regions in partially altered grains.
[2] Chemical analyses of bulk samples of grains.

https://doi.org/10.1346/CCMN.1984.0320504 Published online by Cambridge University Press

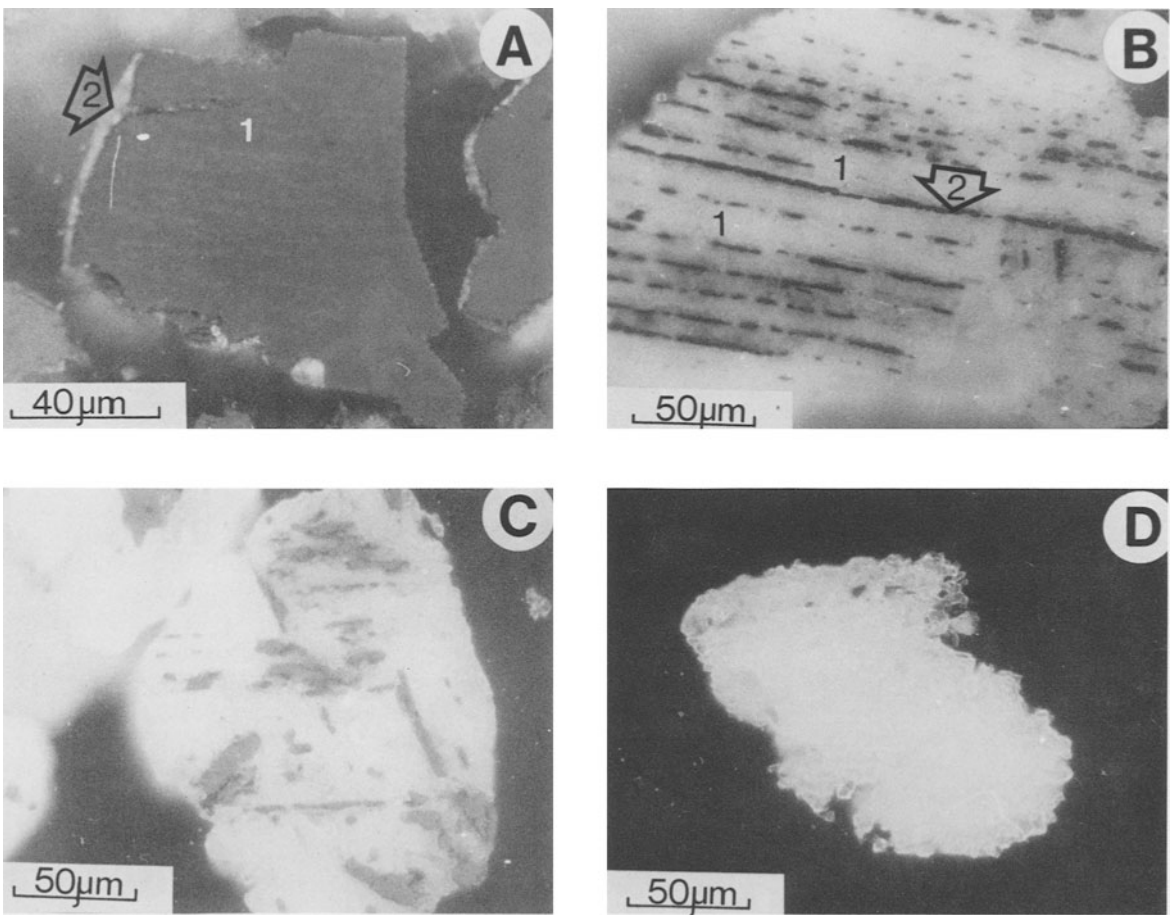

Figure 5. Photomicrographs (reflected light) of polished sections of altered ilmenite grains showing various stages of alteration. (A) Ilmenite with dark grey primary alteration product (pseudorutile) along linear directions (1) and rimmed with secondary alteration product anatase (white) (2). (B) Grain in which anatase zones (1) are separated by parallel bands of isolated ilmenite and/or pseudorutile. (C) Isolated remnants of ilmenite and pseudorutile surrounded by anatase. (D) Leucoxene grain where anatase has completely replaced ilmenite.

crystallization of anatase, and removal of iron by soil solution. The accumulation of Al and Si and the retention of some Fe in completely altered grains were probably due to the presence of impurities in the bulk samples; the probable forms of these elements are discussed below. The analyses of bulk samples of partially and highly altered grains indicate that Cr and V increased whereas Mn, Ni, Zn, Cu, Mg, Co, and Ca decreased during the alteration. The loss of Mn, Cu, Zn, Ni, Co, Ca, and Mg from highly altered grains was probably due to their incompatibility in the crystal structure of anatase; these ions differ from Ti in ionic radius and valency.

Reflected-light photomicrographs of polished sections show that partly altered ilmenite grains consist of a core or bands of a dark grey phase with anatase showing bright yellow internal reflection having developed within and around grains (Figure 5A). The dark grey phase is pseudorutile (Temple, 1966; Ramdohr, 1980). At the intermediate stage of alteration anatase is commonly distributed in bands contained within parallel sheets of original ilmenite/pseudorutile (Figure 5B). Residual ilmenite/pseudorutile is common as small isolated remnants surrounded by anatase (Figure 5C). In the final stages of alteration ilmenite is completely replaced by anatase (Figure 5D).

Scanning electron micrographs of fresh and slightly altered grains show massive, irregular surfaces (Figure 6A). Energy dispersive X-ray spectra from such surfaces (Figure 6B) show the presence of Ti, Fe, and Mn and confirm that the surface material is ilmenite or pseudorutile. Titanomagnetite was not observed in these specimens. Partially altered grains show smooth ilmenite or pseudorutile surfaces covered with fine-grained anatase (Figure 6C). Highly altered grains have very porous surfaces consisting of aggregates (~2 μm) of anhedral particles of anatase and platy to hexagonal crystals of gibbsite and/or kaolinite (1–5 μm) (Figure

https://doi.org/10.1346/CCMN.1984.0320504 Published online by Cambridge University Press

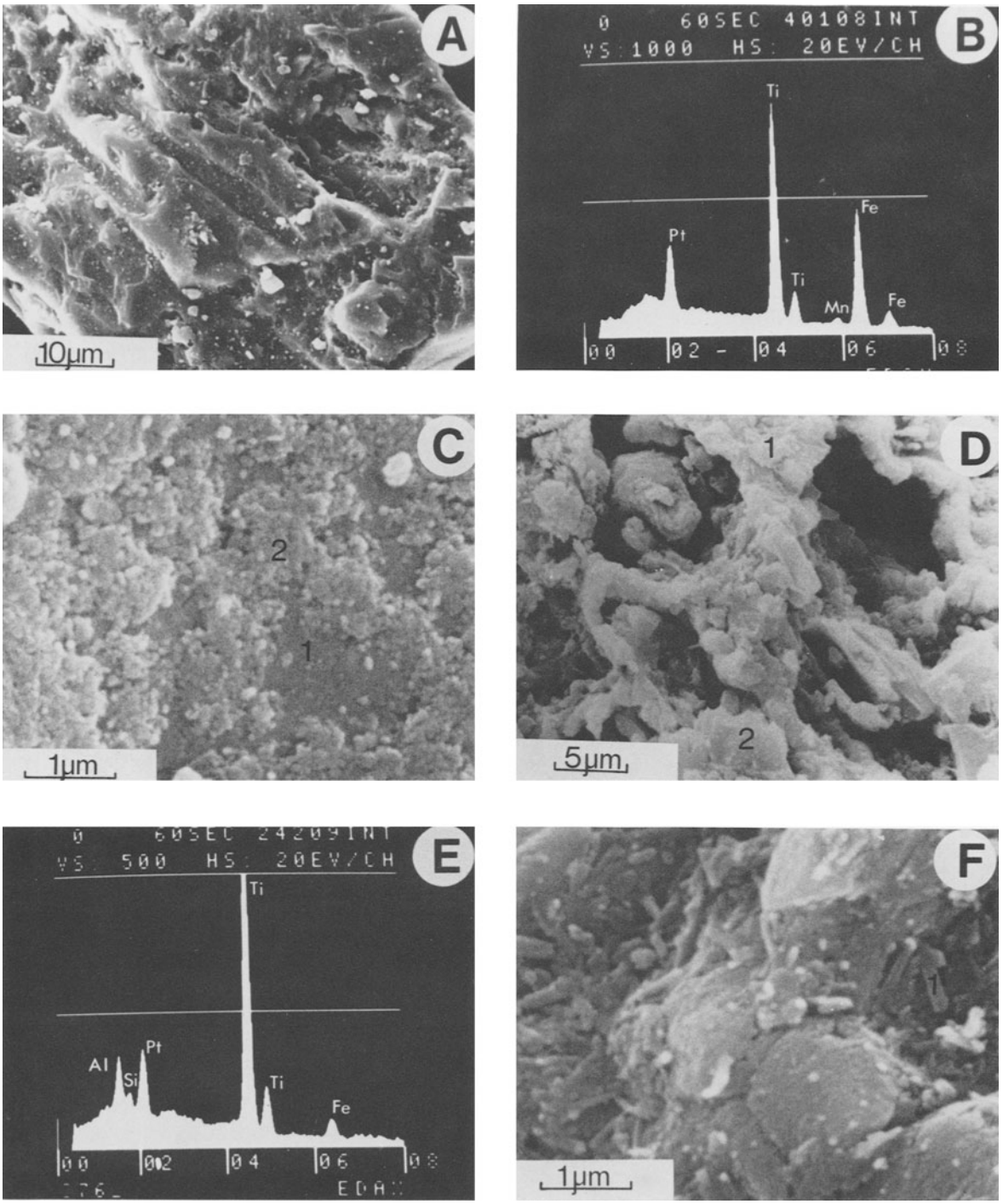

Figure 6. Scanning electron micrographs and energy dispersive X-ray (EDX) spectra of fresh, partially altered, and highly altered ilmenite grains. (A) Fresh ilmenite grain showing massive irregular surface. (B) Spectrum shows the presence of Fe, Ti, and Mn which confirms that the surface material is ilmenite or pseudorutile. Platinum lines are due to the conductive coating. (C) Partially altered grain showing a smooth ilmenite or pseudorutile surface (1) covered with fine-grained alteration products (anatase) (2). (D) Highly altered ilmenite showing a porous framework consisting of aggregates of microcrystalline anatase crystals (1) and platy crystals of kaolinite and/or gibbsite (2). (E) EDX spectrum of surface of grain shown in (D) indicating the presence of much Ti with smaller amounts of Fe, Al, and Si confirming anatase as the major constituent with lesser gibbsite, halloysite and/or kaolinite. (F) Halloysite crystals in voids in a porous microcrystalline anatase framework (1).

https://doi.org/10.1346/CCMN.1984.0320504 Published online by Cambridge University Press

6D). Halloysite (~0.7 μm) apparently crystallized within the porous framework of the altered grain (Figure 6F). EDX spectra (Figure 6E) show the presence of considerable Ti at the surfaces of highly altered grains and lesser amounts of Fe, Al, and Si which are due to the presence of anatase, clay minerals (halloysite, kaolinite), and gibbsite. The presence of these clay minerals and gibbsite within the porous surface is consistent with the mineralogy of the associated pallid-zone clay which is mostly halloysite, kaolinite, and gibbsite.

The retention of the original ilmenite grain shape by its alteration products indicates that isovolumetric weathering has occurred (Millot, 1970). Chemical reactions which describe the alteration of ilmenite to rutile (Grey and Reid, 1975) can be written as:

$$3Fe^{2+}TiO_3 \rightarrow Fe^{3+}{}_2Ti_3O_9 + Fe^{3+}$$
(ilmenite) (pseudorutile) (solid state oxidation)

$$Fe^{3+}{}_2Ti_3O_9 \rightarrow 3TiO_2 + Fe^{3+}{}_2O_3$$
(rutile) (hematite) (dissolution, precipitation)

During the alteration of ilmenite to anatase in the pallid zone most of the Fe was lost to soil solution, whereas in weathered beach sands abundant hematite occurs in leucoxene grains (Grey and Reid, 1975). In the present study no Fe oxides were identified in the leucoxene grains. Thus, alteration of ilmenite in the pallid zone differs from the above model in that anatase is the major product and hematite does not remain within the altered grain.

The porosity of completely altered grains can be calculated from the above equations and the densitites of the minerals. Isovolumetric alteration would produce only 0.65 ml of anatase in 1 ml previously occupied by ilmenite, i.e., the porosity is 35%. This highly porous structure is evident in SEM and microprobe back-scattered electron photographs of altered grains (Figure 6D) with pores ranging from ~100 μm down to the limits of resolution of the techniques (~0.1 μm). These results are consistent with the observations of Lynd (1960) and Temple (1966) who found that altered ilmenites are granular in character and show an increase in porosity with decreasing content of iron.

The identification from SEM photographs and EDX data of the minerals on natural surfaces and fractures of altered grains are tentative because it is based solely on morphology and chemistry. Transmission electron microscopy and electron diffraction were employed to identify alteration products in materials separated from grain surfaces and interiors. Electron micrographs of dispersed, partially altered ilmenite grains show them to consist mostly of anhedral (~0.75 μm) ilmenite and aggregates of ~0.05-μm size particles of anhedral anatase (Figure 7A). In highly altered grains these very small, roughly cylindrical to lath-shaped anatase particles are the major constituents (Figure 7B). They have

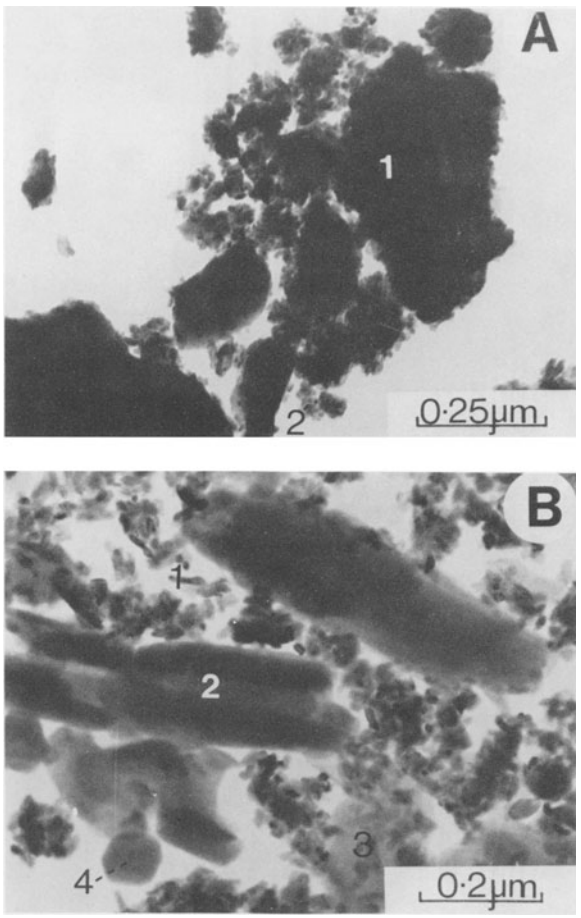

Figure 7. Transmission electron micrographs of <2-μm fraction of altered ilmenite grains. (A) Partially altered ilmenite showing anhedral to subhedral fragments (~0.5 μm) which consist of ilmenite and/or pseudorutile and anatase (1) and fine-grained anatase (2). (B) Highly altered ilmenite showing approximately acicular or lath-shaped (~0.05 μm) anatase crystals (1), tubular halloysite (~0.5 μm) (2), platy crystals of kaolinite (~0.2 μm) (3), and platy, hexagonal crystals (~0.1 μm) which are probably gibbsite (4).

a mean length of 0.06 ± 0.04 μm. Anatase grains were reported to be about 0.1 μm in size in clays and bauxites (Hartman, 1959), 0.2 μm in size in silcrete (Milnes and Hutton, 1974), and 0.2 μm in size in soils (Campbell, 1973). An exception to the generally microcrystalline nature of anatase in soils are the 0.1 mm crystals reported in weathered clays in sandstone (Loughnan and Golding, 1957).

Pseudorutile invariably occurs as anhedral fragments (Figure 8A) and was identified from SAD patterns by its characteristic diffuse reflections (e.g., at 2.78 Å, Figure 8B) that may be assigned to the large, hexagonal, average unit cell described by Grey and Reid (1975). Most reflections are sharp (e.g., at 2.49 Å) and can be assigned to the usual rutile unit cell, but inasmuch as discrete rutile was not present, these reflec-

https://doi.org/10.1346/CCMN.1984.0320504 Published online by Cambridge University Press

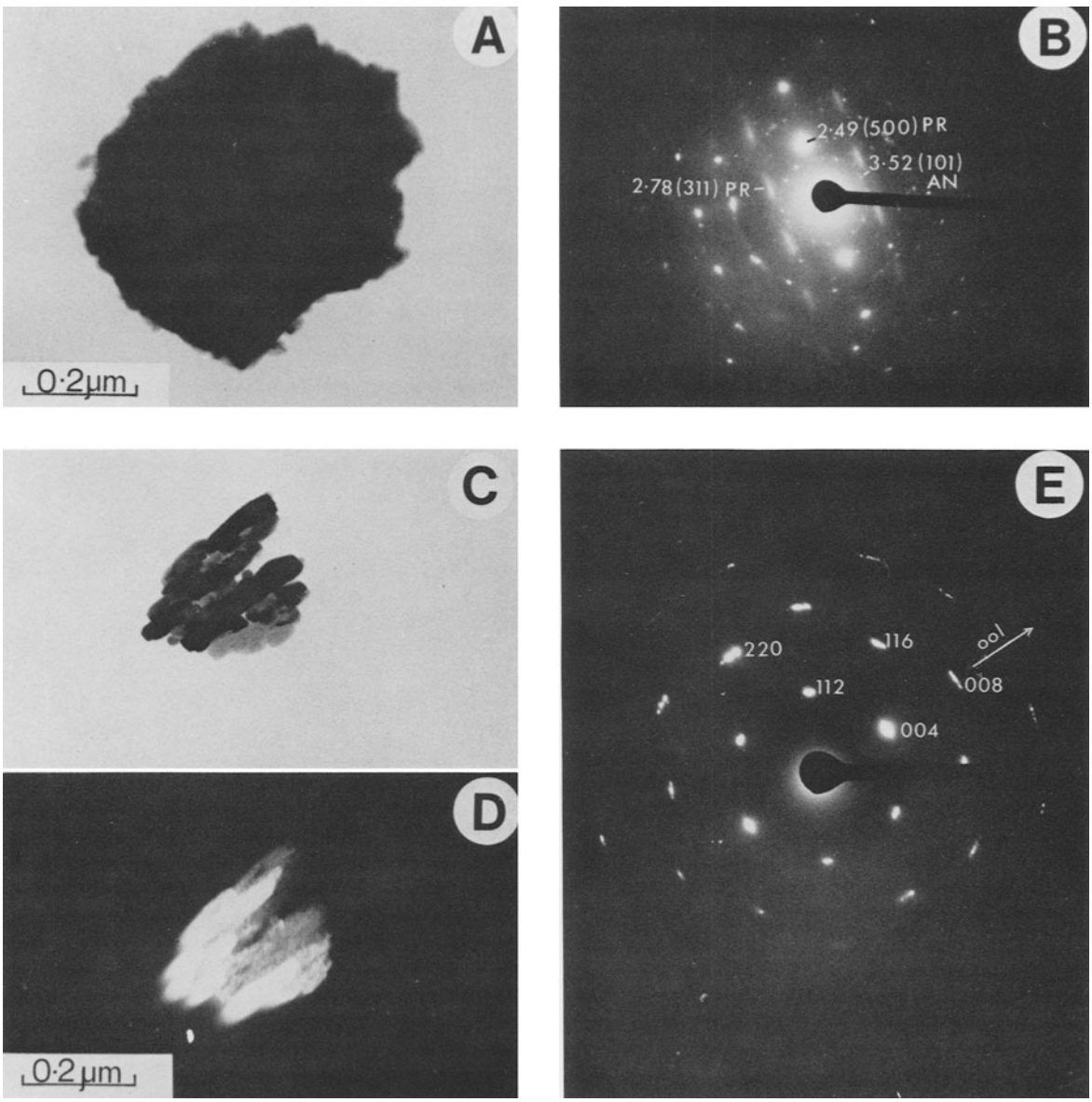

Figure 8. Transmission electron micrograph of an anhedral fragment of pseudorutile (A) and its selected area diffraction (SAD) pattern (B). Indices of reflections due to pseudorutile and anatase are shown. Correctly oriented SAD pattern exhibits characteristic diffuse reflections (2.78 Å) and also sharp reflections (2.49 Å) due to pseudorutile (PR). Spotty ring pattern (3.52 Å) is due to anatase (AN). Bright (C) and dark (D) field micrographs of an aggregate of ~0.1-μm, lath-shaped anatase crystals in a parallel oriented array and their SAD pattern (E) confirming the high degree of orientation. The dark field micrograph was derived from the 004 reflection shown in (E). SAD pattern shows that crystals are elongated along their c-axis.

tions must result from pseudorutile (Brown, 1980). Pseudorutile grains give a single crystal pattern and generally also give a spotty ring pattern (e.g., the 3.52 Å ring in Figure 8B), indicating that several very small anatase particles are present and that anatase did not develop in an oriented epitaxial manner from pseudorutile. This assemblage contrasts with the microcrystalline rutile reported in some altered ilmenites (Teufer and Temple, 1966; Grey and Reid, 1975) which exhibit strong preferred orientation due to epitaxial growth upon the close-packed oxygen sheets of pseudorutile. The anatase structure contains no such well-defined, close-packed oxygen layer (Vegard, 1916), so the potential for epitaxial growth may be absent. Although epitaxial growth on pseudorutile was not observed, anatase crystals were commonly elongated along the c-axis in almost perfectly oriented parallel aggregates (Figures 8C, 8E). The SAD patterns of these ag-

https://doi.org/10.1346/CCMN.1984.0320504 Published online by Cambridge University Press

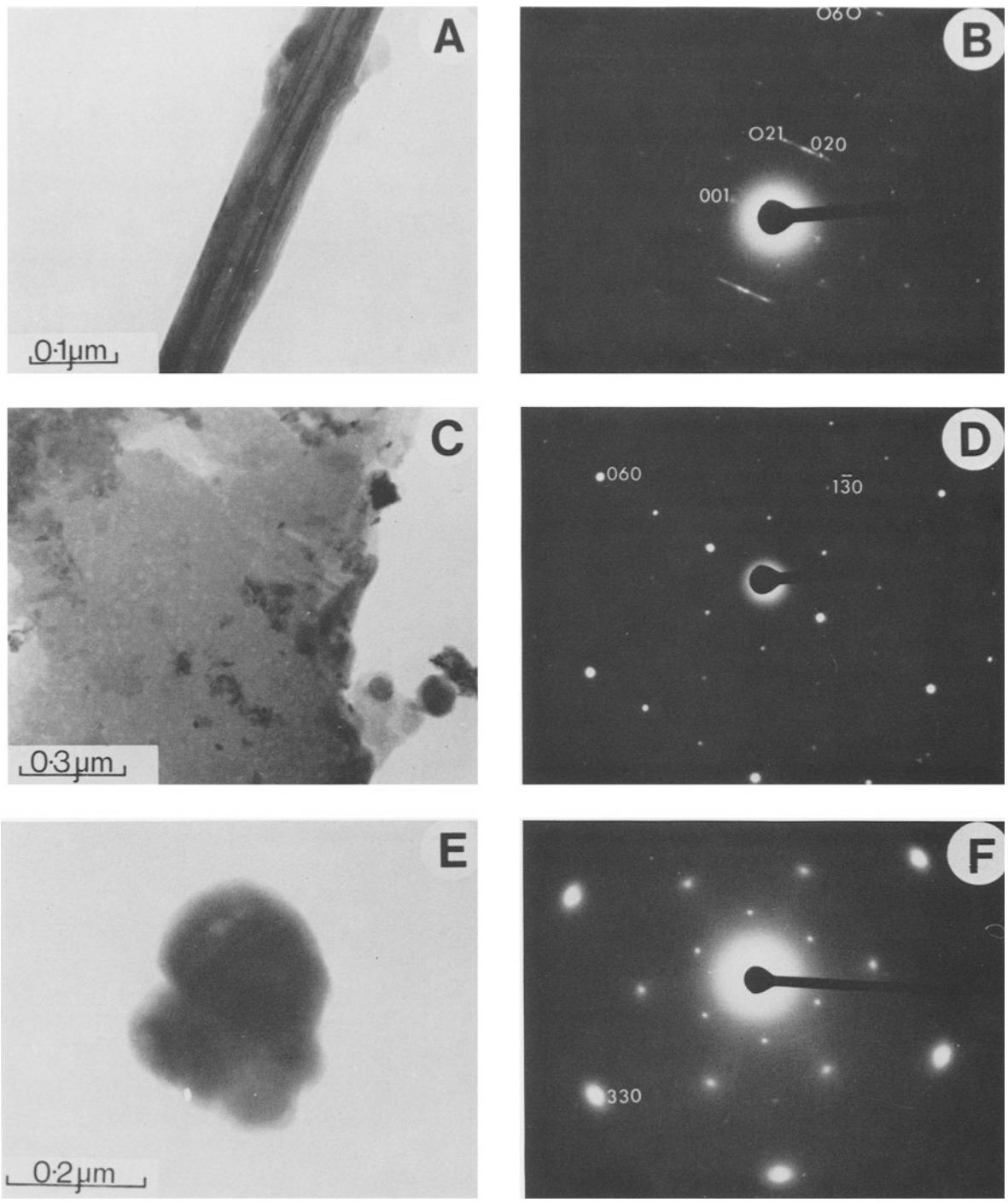

Figure 9. Transmission electron micrographs of halloysite, kaolinite and gibbsite in a dispersed preparation of a highly altered ilmenite (anatase) grain and their selected area diffraction (SAD) patterns. (A) Frayed crystal of tubular halloysite (~0.4 μm long). (B) Its correctly oriented SAD pattern showing that it is elongated along its b-axis. (C) Platy anhedral kaolinite crystal (~2 μm) with a few attached anatase crystals. (D) Its correctly oriented SAD pattern consisting of an hk0 net of reflections with an 060 spacing of 1.49 Å. (E) Anhedral particle (~0.2 μm) of gibbsite. (F) Its correctly oriented SAD pattern consisting of typical slightly arced hk0 reflections with a 330 spacing of 1.46 Å.

https://doi.org/10.1346/CCMN.1984.0320504 Published online by Cambridge University Press

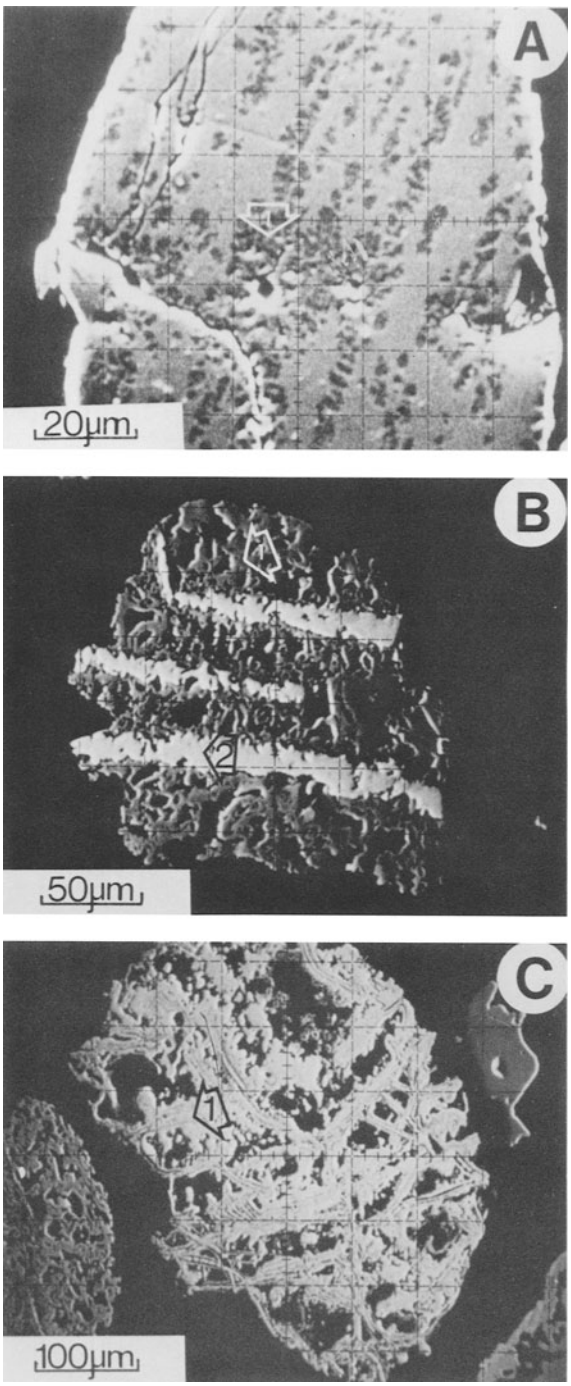

Figure 10. Back scattered electron images of polished sections of altered ilmenite grains. (A) Patchy pseudorutile (1) within ilmenite. (B) Porous framework of anatase (1) separated by approximately parallel zones of unweathered ilmenite and/or pseudorutile (2). (C) A porous framework consisting solely of anatase (1).

gregates consist of hh*l* reflections indicating that the crystals were resting on (110) faces.

The anatase structure (density ~3.4 g/cm³) is much less compact than that of rutile (~4.4 g/cm³) and may be better able to accommodate structural distortions due to foreign ions being incorporated into the crystals from soil solution. The crystallization of anatase rather than rutile may for this reason be a consequence of the presence of the various ions in solution in the pallid-zone weathering environment. In this zone most primary minerals alter and release ions to soil solution. The crystallization of rutile in some beach sands may be due to relatively lower concentrations of ions in soil solution due to the scarcity of easily weathered minerals in these deposits.

Table 3. Average electron microprobe analyses of various regions present in partially altered ilmenite grains.

Wt. %	Ilmenite	Pseudorutile	Anatase
FeO[1]	44.6	34.9	5.0
TiO_2	52.3	57.3	88.6
Mn_2O_3	3.2	2.3	0.02
SiO_2	0.0	0.0	0.58
Al_2O_3	0.07	0.39	2.1

[1] Expressed as FeO; most iron is oxidized in pseudorutile and anatase regions.

Halloysite crystals within highly altered ilmenite grains are distinctly tubular in shape but have a somewhat irregular outline (average length = 0.4 ± 0.1 μm; width = 0.1 ± 0.004 μm). These crystals are generally slightly shorter than the halloysite in the pallid-zone matrix which has an average length of 0.7 ± 0.4 μm and a width of 0.1 ± 0.04 μm. This difference may be a consequence of the restricted space for crystal growth within pores in the altered ilmenite grain. SAD patterns show that halloysite crystals are mostly elongated along their b-axis (Figure 9A, 9B) as in the matrix. Honjo *et al.* (1954) also found that most halloysite crystals in Hong Kong kaolin are elongated along their b-axis.

Some kaolinite occurs as large (>2 μm) anhedral grains within the anatase matrix (Figure 9C). The electron diffraction pattern of kaolinite consists of a hk0 net of reflections with an 060 spacing of 1.49 Å (Figure 9C). Gibbsite usually occurs as anhedral grains (~0.4 μm) that give typical, slightly arced hk0 reflections (Figures 9E, 9F) with a 330 spacing of 1.46 Å.

An examination of weathered ilmenite grains from Western Australian beach sands showed that halloysite, kaolinite, and gibbsite occur within grains in an identical manner to the grains from the pallid zone described above. This is a significant result inasmuch as existing methods of beneficiating the ore are based on the assumption that Al and Si impurities are substituted in rutile or anatase. Because most of the Al and Si has been shown to be present as discrete clay minerals and gibbsite, these elements may be removed by caustic leaching procedures that do not dissolve the titanium oxides.

https://doi.org/10.1346/CCMN.1984.0320504 Published online by Cambridge University Press

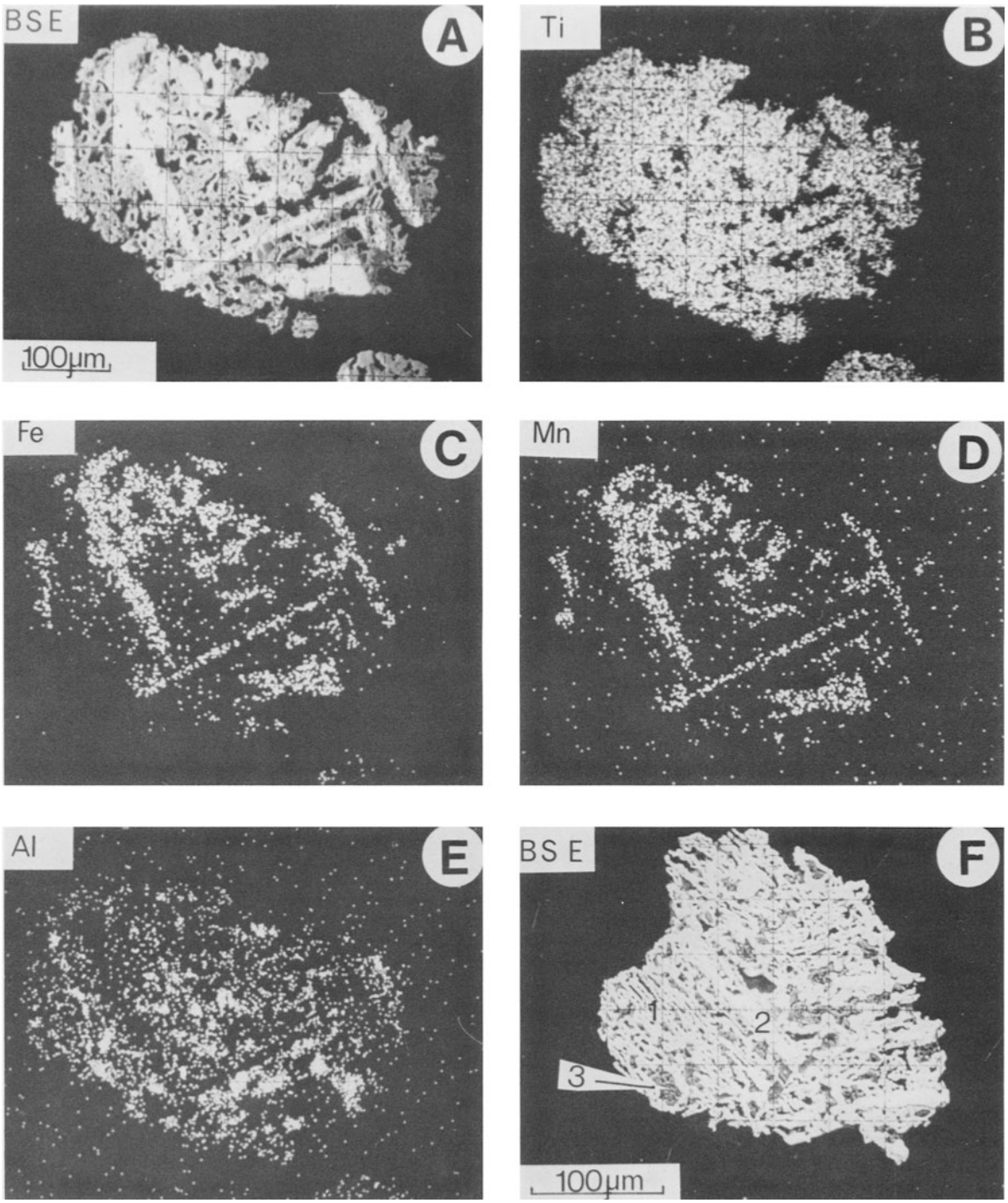

Figure 11. Electron microprobe X-ray images of partially altered ilmenite grains showing zones of ilmenite/pseudorutile and anatase. The association of Ti, Fe, and Mn in the residual ilmenite/pseudorutile zones and the absence of Fe and Mn and presence of Al in anatase zones (B, C, D, E) are shown. The presence of Al within the porous anatase matrix is due to crystallization of halloysite, kaolinite, and gibbsite from soil solution. (F) Highly altered grain showing a porous arrangement of anatase (1) with isolated remnants of ilmenite and pseudorutile (2). The pores within the porous framework of anatase are filled by a mixture of 56% gibbsite and 44% kaolinite and/or halloysite (3). BSE = Back scattered electron images.

https://doi.org/10.1346/CCMN.1984.0320504 Published online by Cambridge University Press

Chemical composition of individual altered grains

The patchy development of pseudorutile along linear directions in partly altered ilmenite is clearly seen in electron microprobe back-scattered electron images (Figure 10A). In partly altered grains anatase is common in zones aligned parallel with bands of the original ilmenite/pseudorutile (Figure 10B) so that ilmenite/pseudorutile remnants are surrounded by porous anatase. In highly altered (leucoxene) grains, ilmenite has been completely replaced by a porous arrangement of microcrystalline anatase (Figure 10C). A similar porous fabric was described by Ramdohr (1980) in altered ilmenite from Sweden. Average concentrations of Fe, Ti, Si, Al, and Mn in various regions of partly altered grains are given in Table 3. These data show an increase in titanium and a loss of iron with increasing alteration of ilmenite grains of average formula ($Fe^{2+}_{0.93}Ti^{4+}_{0.99}Mn^{3+}_{0.06}O_3$) to anatase ($TiO_2$) through pseudorutile ($Fe^{3+}_{1.99}Ti^{4+}_{2.92}Mn^{3+}_{0.12}O_9 \equiv M_{5.03}O_9$). Structural formulae of ilmenite and pseudorutile were calculated on the basis of 3 and 9 oxygen atoms, respectively, and on the assumption that all of the Fe in ilmenite is present as Fe^{2+} and in pseudorutile as Fe^{3+}. Grey and Reid (1975) published a structural formula for a South Australian pseudorutile, ($Fe^{3+}_{1.81}Fe^{2+}_{0.07}Mn^{3+}_{0.03}Ti^{4+}_{3.08}O_9 \equiv M_{4.99}O_9$ (excluding H_2O)), and an Indonesian pseudorutile, ($Fe^{3+}_{1.34}Fe^{2+}_{0.26}Mn^{3+}_{0.15}Ti^{4+}_{3.25}O_9 \equiv M_{5.00}O_9$ (excluding H_2O)). The structural formula obtained in the present study is close to the former.

Some Mn was apparently lost during the alteration of ilmenite to pseudorutile, and the rest was lost during the subsequent alteration to anatase. The presence of Mn in ilmenite and pseudorutile and its absence in anatase is seen in the electron probe element distribution maps of partly altered grains (Figure 11D), confirming the interpretation of analyses of bulk materials described above. Evidently, Mn substitutes for Fe in ilmenite and pseudorutile but not for Ti in anatase. Al appears to be absent in ilmenite and pseudorutile but present in patches of clay within the porous anatase matrix (Figure 11E). Si and Al are only minor constituents of ilmenite but are abundant in bulk samples of completely altered grains (Table 2). These results agree with those of Frost *et al.* (1983) for partly altered ilmenite grains in mineral sand deposits where Si and Al increased with decreasing Fe within altered regions of grains having average compositions between rutile and pseudorutile. These authors considered that during the latter stages of ilmenite alteration, where rutile crystallizes from solution, both alumina and silica are extracted from the ambient environment and are coprecipitated with, or adsorbed on, rutile. In the lateritic pallid zone studied in the present investigation, the altered grain simply acted as a continuation of the porous soil matrix and was pervaded by soil solution from which the clay of the pallid zone crystallized. The pores within the anatase grains are commonly filled with clay minerals and gibbsite (Figure 11F). Microprobe analysis of clay-filled regions within anatase grains (such as region 3 in Figure 11F) gave average values of 20% SiO_2 and 54% Al_2O_3. These values are consistent with a mixture of gibbsite (56%) and halloysite and/or kaolinite (44%) and are similar to the composition of the clay fraction of the matrix (i.e., ~40% gibbsite, 60% halloysite and/or kaolinite).

Mechanism of ilmenite weathering in lateritic pallid zone

Grey and Reid (1975) reported that the alteration of ilmenite is a 2-stage process. First, all of the iron oxidizes, and some diffuses from the ilmenite leaving pseudorutile in which closely packed oxygen layers remain intact. This stage of the alteration is represented by the following reaction:

$$3Fe^{2+}{}_2TiO_3 \rightarrow Fe^{3+}{}_2Ti_3O_9 + Fe^{3+}.$$

In the second stage of alteration pseudorutile dissolves, iron is removed by solution, and TiO_2 precipitates rapidly. The second stage involves a disruption of the oxygen packing as both iron and oxygen are removed and is represented by the following reaction:

$$Fe^{3+}{}_2Ti_3O_9 \rightarrow 3TiO_2 + Fe_2O_3.$$

They considered that epitaxial growth of TiO_2 crystals (rutile in their example) occurs on a pseudorutile substrate so that the primary ilmenite grain is replaced by a highly oriented array of rutile microcrystals.

The results of the present study differ from Grey and Reid's (1975) findings in three major respects which reflect the different weathering environments in beach sand deposits compared with a lateritic pallid zone. First, anatase and *not* rutile was the final alteration product. Second, anatase crystals did *not* crystallize in parallel alignment throughout the former ilmenite grain; they were found in parallel orientation, but these aggregates were of limited extent only. Third, the high porosity of the anatase grain appears to have enabled halloysite, kaolinite, and gibbsite to crystallize from soil solution within pores.

ACKNOWLEDGMENTS

We are grateful to Terry Armitage and John Hillyer for their assistance with electron optical techniques, and to Drs. J. Graham, D. Morris, I. Grey, and A. Milnes for helpful discussions.

REFERENCES

Bailey, S. W., Cameron, E. M., Spedden, H. R., and Weege, R. J. (1956) The alteration of ilmenite in beach sands: *Econ. Geol.* **51**, 263–279.

Brown, G. (1980) Associated minerals: in *Crystal Structure of Clay Minerals and their X-ray Identification*, G. W.

Brindley and G. Brown, eds., Mineral. Soc., London, 361–411.

Bykov, A. D. (1964) Proarizonite as a secondary mineral due to supergene alteration of ilmenite: *Dokl. Akad. Nauk S.S.S.R.* **156,** 567–570.

Campbell, A. S. (1973) Anatase and rutile determination in soil clays: *Clay Miner.* **10,** 57–58.

Deer, W. A., Howie, R. A., and Zussman, J. (1962) *Rock Forming Minerals, Vol. 5. Non-silicates:* Longmans, London, 28–33.

Flinter, B. H. (1959) The alteration of Malayan ilmenite grains and the question of "arizonite": *Econ. Geol.* **54,** 720–729.

Frost, M. T., Grey, I. E., Harrowfield, I. R., and Mason, K. (1983) The dependence of alumina and silica contents on the extent of the alteration of weathered ilmenites from Western Australia: *Mineral. Mag.* **47,** 201–208.

Gandolfi, G. (1967) Discussion upon methods to obtain X-ray powder patterns from a single crystal: *Mineral. Petrogra. Acta* **13,** 67–74.

Grey, I. E. and Reid, A. F. (1975) The structure of pseudorutile and its role in the alteration of ilmenite: *Amer. Mineral.* **60,** 898–906.

Hartman, J. A. (1959) The titanium mineralogy of certain bauxites and their parent minerals: *Econ. Geol.* **54,** 1380–1405.

Honjo, G., Kitamura, N., and Mihama, K. (1954) Study of clay minerals by single crystal electron diffraction diagrams—The structure of tubular kaolin: *Clay Miner. Bull.* **2,** 131–141.

Karkhanavala, M. D. (1959) The nature of arizonite. *Econ. Geol.* **54,** 1302–1308.

Lee, R. F. and McConchie, D. M. (1982) Comprehensive major and trace element analysis of geological material by X-ray fluorescence, using low dilution fusion: *X-ray Spectrometry* **11,** 55–63.

Loughnan, F. C. and Holding, H. G. (1957) The mineralogy of the commercial dyke clays in the Sydney district, New South Wales: *J. Proc. R. Soc. N.S.W.* **91,** 85–91.

Lynd, L. E. (1960) Alteration of ilmenite: *Econ. Geol.* **55,** 1064–1070.

Millot, G. (1970) *Geology of Clays:* Springer-Verlag, Berlin, 429 pp.

Milnes, A. R. and Hutton, J. T. (1974) The nature of microcryptocrystalline titania in silcrete skins from the Beda Hill area of South Australia: *Search* **5,** 153–154.

Palmer, C. (1909) Arizonite, ferric metatanate: *Amer. J. Sci.* **28,** 353–356.

Ramdohr, P. (1980) *The Ore Minerals and their Intergrowths:* Vol. 2, Pergamon Press, Oxford, 1207 pp.

Sadleir, S. B. and Gilkes, R. J. (1976) Development of bauxite in relation to parent material near Jarrahdale, Western Australia: *J. Geol. Soc. Aust.* **23,** 333–344.

Temple, A. K. (1966) Alteration of ilmenite: *Econ. Geol.* **61,** 695–714.

Teufer, G. and Temple, A. K. (1966) Pseudorutile, a new mineral intermediate between ilmenite and rutile in the natural alteration of ilmenite: *Nature* **211,** 179–181.

Van Houten, F. B. (1968) Iron oxides in red beds: *Bull. Geol. Soc. Amer.* **79,** 399–416.

Vegard, L. (1916) Results of crystal analysis: *Phil. Mag. Ser. 6* **32,** 505.

Vogel, A. I. (1961) *A Textbook of Quantitative Inorganic Analyses:* Longmans, London, 856 pp.

(Received 15 September 1983; accepted 6 March 1984)

Резюме—В латеритовой бледной зоне кристаллы ильменита видоизменяются через псевдорутил в зерна пористого лейкоксена, состоящие из агрегатов беспорядочно ориентированных ~0,6 μм кристаллов анатаза. Этот тип видоизменения отличается от типа в пляжных песках, в которых параллельно ориентированные кристаллы рутилов развиваются из псевдорутилов. Увеличенное содержание Si и Al в видоизмененных зернах обусловлено кристаллизацией галлуазита, каолинита и гиббсита из почвенного раствора внутри пор скорее, чем в результате включения этих элементов в кристаллы анатаза. Марганец являлся значительным составным элементом (3,2% Mn_2O_3) первоначального ильменита, но не удерживался зернами лейкоксена. Второстепенные составные элементы Ni, Zn, Cu, Mg, Co, и Ca были также потеряны, но Cr и V удерживались. [E.G.]

Resümee—In einer lateritischen palliden Zone wandeln sich Ilmenitkristalle über Pseudorutil in poröse Leucoxenkörner um, die aus Aggregaten von unregelmäßig angeordneten etwa 0,6 μm großen Anataskristallen bestehen. Diese Umwandlungsart unterscheidet sich von der in Küstensanden, wo sich parallel orientierte Rutilkristalle aus dem Pseudorutil bilden. Eine Zunahme des Si- und Al-Gehaltes in den umgewandelten Körnern rührt eher von der Kristallisation von Halloysit, Kaolinit und Gibbsit in den Poren aus der Porenlösung her als vom Einbau dieser Elemente in die Anataskristalle. Mangan war in beachtlichen Mengen (3,2% Mn_2O_3) im ursprünglichen Ilmenit enthalten, wurde aber durch die Leucoxenkörner nicht zurückgehalten. Die Spurenelemente Ni, Zn, Cu, Mg, Co, und Ca gingen ebenfalls verloren, während Cr und V zurückgehalten wurden. [U.W.]

Résumé—Dans une zone ilménite latérite pâle, des cristaux sont altérés via la pseudorutile en grains leucoxènes poreux composés d'aggrégats de cristaux d'anatase de ~0,6 μm orientés au hasard. Ce style d'altération diffère de celui du sable de plage où des cristaux de rutile orientés parallèlement se développent à partir de la pseudorutile. L'élévation du contenu en Si et Al dans les grains altérés est due à la cristallisation à partir de solutions du sol d'halloysite, de kaolinite, et de gibbsite endéans les pores plutôt qu'à l'incorporation de ces éléments dans les cristaux anatase. La manganèse était un constituent significatif (3,2% Mn_2O_3) de l'ilménite originale, mais n'a pas été retenue par les grains leucoxènes. Les constituents mineurs Ni, Zn, Cu, Mg, Co, et Ca ont aussi été perdus, mais Cr et V ont été retenus. [D.J.]